ACS Macro Letters

Letter

pubs.acs.org/macroletters

Highly Luminescent Polymer Particles Driven by Thermally Reduced Graphene Quantum Dot Surfactants

Hyunseung Yang,[†] Dong Jin Kang,[†] Kang Hee Ku,[†] Han-Hee Cho,[†] Chan Ho Park,[†] Junhyuk Lee,[†] Doh C. Lee,[†] Pulickel M. Ajayan,[‡] and Bumjoon J. Kim*[,†]

[†]Department of Chemical and Biomolecular Engineering, Korea Advanced Institute of Science and Technology (KAIST), Daejeon 305-701, Republic of Korea

[‡]Department of Mechanical Engineering and Materials Science, Rice University, Houston, Texas 77005-1892, United States

Supporting Information

ABSTRACT: We report the use of highly luminescent graphene quantum dots (GQDs) as efficient surfactants to produce Pickering emulsions and novel polymer particles. To generate the GQD surfactants, the surface properties of 10 nm sized, non-reduced GQDs (nGQDs), which have strong hydrophilicity, were synthesized and modified in a systematic manner by the thermal reduction of oxygen-containing groups at different treatment times. In stark contrast to the behavior of the nGQDs, thermally reduced GQDs (rGQDs) can produce highly stable Pickering emulsions of oil-in-water systems. To demonstrate the versatility of the rGQD surfactants, they were applied in a mini-emulsion polymerization system that requires nanosized surfactants to synthesize submicron-sized polystyrene particles. In addition, the use of rGQD surfactants can be extended to generating block copolymer particles with controlled nanostructures. Particularly, the polymer particles were highly luminescent, a characteristic produced by the highly fluorescent GQD surfactants, which has great potential for various applications, including bioimaging, drug delivery, and optoelectronic devices. To the best of our knowledge, this is the first report in which nanosized GQDs were used as surfactants.

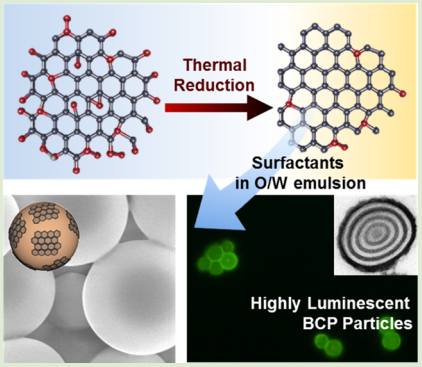

Pickering emulsions stabilized by particles hold great promise for use in cosmetics, pharmaceutical formulations, and other novel colloid-based materials.[1−3] In contrast to conventional surfactants, particle surfactants exhibit highly stable, quasi-irreversible adsorption to the oil−water interfaces, thus producing emulsions that are stable against coalescence.[2,4−7] Recently, graphene oxide (GO) has been used as a particle surfactant because of its amphiphilicity,[8−14] which provides strong adsorption to the oil−water interface. However, practical applications of the GO surfactants for producing emulsions, particularly in bioimaging and optical applications, have been limited because they do not possess luminescent properties. Moreover, GO sheets are not typically suitable for producing submicron-sized emulsion droplets due to the curvature effect caused by their large size, which is in stark contrast to the nanosized metal and polymeric particle surfactants.[15−26]

Recently, graphene-based semiconductor nanoparticles (NPs), also termed graphene quantum dots (GQDs), have attracted significant attention as a new type of luminescent NPs because of their remarkable physical, mechanical, and optoelectronic properties.[27−34] In addition, GQDs are free of toxic metal atoms and thus are considered to be environmentally benign, making them more suitable for use in biological and optoelectronic devices than other fluorophores, including inorganic quantum dots.[35−38] Therefore, if the surface properties of the GQDs can be precisely and reproducibly controlled, they hold great promise as efficient surfactants for developing new emulsion-based materials. In particular, the efficiency of GQDs as surfactants can be greatly amplified due to their nanosized dimensions and high surface-to-volume ratio compared to that of micron-sized GO sheets. In addition, the unique photoluminescent properties and biocompatibility of GQDs can extend the range of applications for GQD-stabilized emulsions to bioimaging and drug-delivery systems.[30,35,39] Despite such extraordinary potentials of GQDs as surfactants, to the best of our knowledge, they have never been used for this purpose because of the difficulty of obtaining the desired surface properties. Whereas large GO sheets typically have a well-balanced amphiphilicity with hydrophilic edges and hydrophobic π domains on the basal plane,[40−43] the surface properties of the GQDs are dominated by their large portion of hydrophilic edges. Recently, it was reported that the hydrophilic oxygen content of GQDs could be tailored by using thermal treatment and chemical-grafting approaches.[37,39] In comparison with the chemical-grafting approach, the thermal treatment method can control the degree of reduction by tuning the treatment time, thus providing better control of the

Received: June 26, 2014
Accepted: September 8, 2014
Published: September 12, 2014

 © 2014 American Chemical Society dx.doi.org/10.1021/mz5003855 | *ACS Macro Lett.* 2014, 3, 985−990

Scheme 1. Schematic Illustration of the Preparation of GQD Surfactants via the Thermal Reduction Method and Their Application As Surfactants in O/W Emulsion Systems[a]

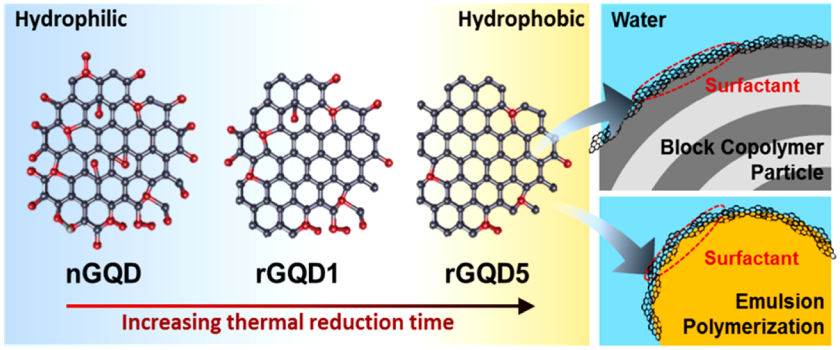

[a]Controlling the amphiphilicity of the GQDs, which can be accomplished by varying the thermal reduction time, was essential in determining their capability to function as nanosurfactants.

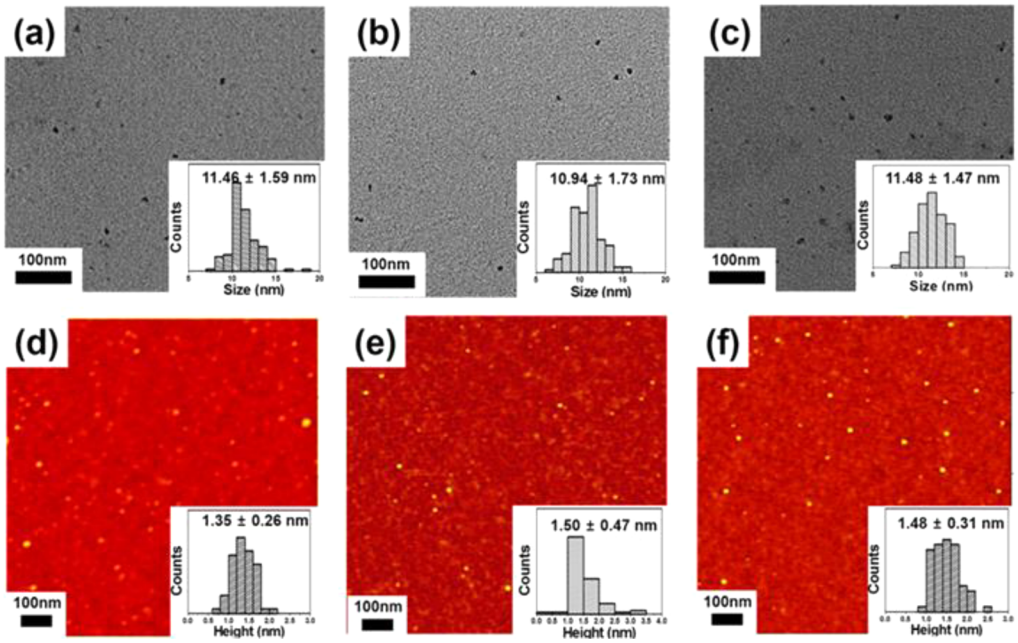

Figure 1. TEM images of GQDs and the corresponding histograms of their size distributions: (a) nGQD, (b) rGQD1, (c) rGQD5; AFM images of GQDs and the corresponding histograms of their height distributions: (d) nGQD, (e) rGQD1, (f) rGQD5.

surface properties of the GQDs with relatively small particle-to-particle deviation.

In this work, we developed GQD surfactants with tailored amphiphilicity via the thermal reduction method, and we used them to produce highly stable oil/water (O/W) emulsions (Scheme 1). In order to prepare a series of GQDs of the same size that have different amphiphilicities, the GQDs were thermally reduced at different exposure times, ranging from 0 to 7 days, at 150 °C. Therefore, we removed significant quantities of the hydrophilic oxygen-containing groups on the surface while retaining the hydrophobic basal plane, giving the GQDs the desired amphiphilicity for use in efficient surfactants. Then, we used them as surfactants for the mini-emulsion polymerization of styrene and for producing block copolymer (BCP) particles through the "emulsion-encapsulation and evaporation process". It was observed that only the GQDs that were thermally reduced for more than 5 days had the desired surface properties and functioned successfully as surfactants in the systems. These BCP particles were highly luminescent, demonstrating a successful example of the synergistic combination of the unique properties of the GQDs into the composites.

To produce the GQD surfactants, first, we synthesized the GQDs by using the method reported previously.[32,44] Figures 1(a) and (d) show that the GQDs were monodispersed with the size of 11.46 ± 1.59 nm, and their average height was 1.35 ± 0.26 nm, suggesting that they were mostly single-layered or bilayered.[27] High-resolution TEM images showed that the GQDs had a crystalline structure with a lattice parameter of 0.24 nm (Figure S1, Supporting Information). Then, the thermal reduction approach was used to remove the oxygen-containing groups on the GQDs, producing reduced GQDs (rGQDs). Since the prevalence of oxygen-containing groups is a critical parameter that determines the amphiphilicity of the GQDs, we prepared five different GQDs with thermal reduction times of 0, 1, 3, 5, and 7 days, respectively. For convenience, we denoted them as nGQD, rGQD1, rGQD3, rGQD5, and rGQD7, respectively. After the thermal reduction

dx.doi.org/10.1021/mz5003855 | ACS Macro Lett. 2014, 3, 985−990

process, all of the rGQDs were well dispersed in various solvents without any aggregation or change in size. For example, the TEM and AFM images of nGQDs, rGQD1s, and rGQD5s in Figure 1 show that the GQDs had nearly identical sizes and heights before and after thermal reduction.

We performed high-resolution C 1s X-ray photoelectron spectroscopy (XPS) analysis to monitor the reduction of the GQDs and change in their chemical structure during the thermal reduction process. The XPS spectrum of the nGQDs in Figure 2 shows peaks at 284.5, 285.6, and 289.2 eV, confirming

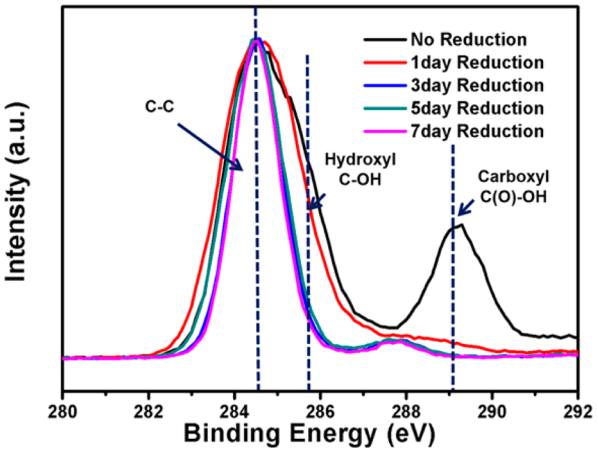

Figure 2. XPS C 1s spectra of nGQD, rGQD1, rGQD3, rGQD5, and rGQD7.

the presence of graphitic networks, hydroxyl groups, and carboxyl groups, respectively.[45] The intensities of the peaks at 285.6 and 289.2 eV in Figure 2 were compared to monitor the progress of the thermal reduction process. The peaks of the rGQDs at 285.6 and 289.2 eV decreased gradually as the thermal reduction time increased from 0 to 5 days, which indicated that the hydroxyl and carboxyl groups on the GQDs were being removed effectively. Upon thermal reduction, the graphitic network peak of the rGQDs became narrower than that of the nGQDs. This feature provides additional evidence for the preservation of the graphitic basal plane and the successful thermal reduction process.[45,46]

Attenuated total reflectance-Fourier transform infrared (ATR-FTIR) characterization was performed to provide further evidence of effective thermal reduction (Figure S2, Supporting Information). Strong signals of hydroxyl (3300 cm^{-1}) and carboxyl (1720 cm^{-1}) functional groups were observed for nGQDs, which is consistent with previous reports.[35] However, the intensities of the peaks at 3300 and 1720 cm^{-1} decreased, which was attributed to the removal of the hydroxyl and carboxyl groups during the thermal reduction process. To obtain a quantitative comparison of the reduction effect in relation to the thermal reduction time, the total atomic ratio of C/O in the GQD samples was calculated from the XPS data, and the results are summarized in Table S1 (Supporting Information). In detail, the C/O ratios had an increasing trend as a function of thermal treatment time, i.e., 2.11 (nGQD), 7.55 (rGQD1), 16.47 (rGQD3), and 17.33 (rGQD5), which indicated that oxygen-containing groups (i.e., hydroxyl and carboxyl groups) were gradually being removed and that the hydrophobicity of the GQDs was increased during the thermal reduction process.[45] The C/O ratios were saturated after 5 days of thermal reduction. Variations in hydrophobicity can be evaluated by monitoring the contact angle measurements of the GQDs as a function of thermal treatment time (Figure S3, Supporting Information). The diiodomethane contact angle decreased in the order of nGQD, rGQD1, and rGQD5, ranging from 29.6° to 16.1°, indicating that the hydrophilicities of the GQDs' surfaces were reduced significantly. Therefore, a delicate balance in the amphiphilicities of the surface properties of the rGQDs can be achieved simply by tuning the length of time they are subjected to the thermal reduction process.

To examine the potential of thermally reduced GQDs as surfactants in O/W emulsions, a series of samples consisting of toluene/water mixtures (1/1 mL) were prepared, and different types of GQDs, i.e., nGQD, rGQD1, and rGQD5, were added to the mixtures, followed by vigorous shaking for 1 min. In each solution, the concentration of the GQDs was fixed at 1 mg/mL. The morphologies of each different mixture were compared 72 h after the preparation. Figure 3 shows representative photographic images of the toluene/water mixtures that contained (a) nGQD, (b) rGQD1, and (c) rGQD5. When nGQDs or rGQD1s were added, they stayed in the water phase, and no Pickering emulsions were created, even after vigorous shaking (Figure 3(a) and (b)). In contrast, the addition of rGQD5s created an emulsified layer of micron-sized toluene/water droplets that were extremely stable for several months (Figure 3(c) and (d)). Thus, it indicated that the rGQD5s were adsorbed strongly to the toluene/water interface, acting as efficient surfactants that modify the interfacial and morphological properties of the emulsions by reducing the interfacial tension.[8] These results can be explained by the difference of the adsorption energy (E_a) of the particles onto the interface between the oil and water phases, as expressed by the following equation[47,48]

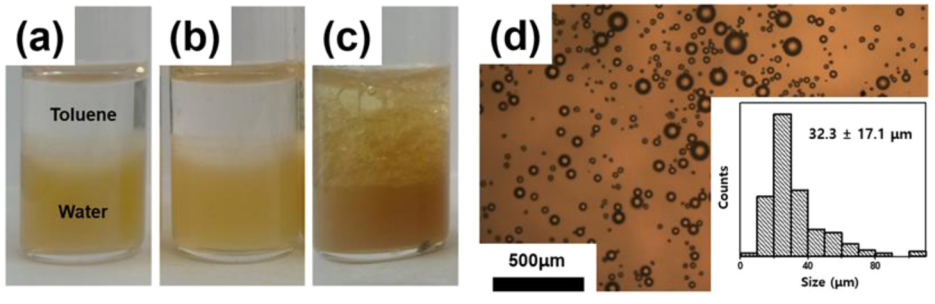

Figure 3. Photographic images of toluene/water mixtures containing different GQDs: (a) nGQD, (b) rGQD1, and (c) rGQD5. Only the addition of rGQD5 produced stable toluene-in-water Pickering emulsions. (d) Optical microscopic images of toluene-in-water Pickering emulsions stabilized by rGQD5. The inset is a histogram of the size distribution of the emulsion droplets.

dx.doi.org/10.1021/mz5003855 | ACS Macro Lett. 2014, 3, 985−990

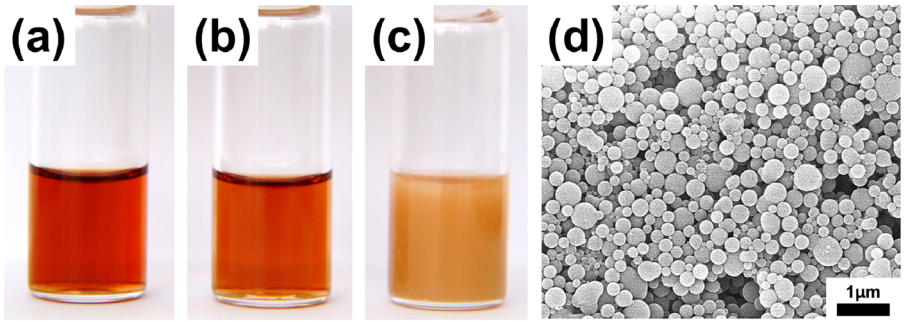

Figure 4. Photographic images of solutions after mini-emulsion polymerization with the addition of (a) nGQD; (b) rGQD1; and (c) rGQD5 (only rGQD5 produced stable, milky-brown emulsions). (d) SEM images of micron-sized, stable PS colloidal particles stabilized by rGQD5.

$$E_a = (\pi R^2 \gamma_{oil-water})(1 - |\cos(\theta)|)^2$$

where

$$|\cos(\theta)| = \frac{|\gamma_{particle-oil} - \gamma_{particle-water}|}{\gamma_{oil-water}} \quad (1)$$

where R is the radius of the particles; γ_{1-2} is the interfacial tension between component 1 and component 2; and $\cos(\theta)$ is the ratio of the difference in the interfacial tension between the particles and the oil and water to that between the oil and the water. Therefore, the surfactant efficiency is a function of the particle size and of the surface properties of the particles. Because nGQD and rGQDs had the same size as shown in Figure 1, the surface properties of the GQDs should be the sole parameter that determines the efficiency of the GQDs as surfactants in the emulsion system. It was predicted that rGQDs have smaller $\cos(\theta)$ as well as higher E_a when they have balanced amphiphilicity. Therefore, rGQD5s, with much stronger hydrophobicity than nGQDs and rGQD1s, are preferentially adsorbed to the interface rather than being dissolved in the water phase. To investigate the efficiency of the rGQD5 surfactant, the number-average size of emulsion droplets and their size distribution were obtained by analysis of optical microscopic images, counting at least 300 droplets. The statistics are shown in the corresponding histograms as an inset in Figure 3(d). The average size of the droplets was determined to be 32.3 ± 17.1 μm. In comparison with the case where the micron-sized GO was used as surfactant, rGQD5 produced much smaller toluene/water droplets under similar emulsion preparation conditions.[8] Therefore, the efficiencies of the GQD surfactants can be enhanced significantly due to their nanosized dimensions compared to those by micron-sized GO sheets.

To demonstrate the potential of rGQD surfactants for producing emulsion-based materials, mini-emulsion polymerization of styrene was performed using three different GQDs, i.e., nGQD, rGQD1, and rGQD5, as surfactants for 24 h at 70 °C. When polymerization was performed with nGQD and rGQD1, no formation of PS colloidal particles was observed (Figures 4(a) and (b)). Interestingly, when rGQD5s were used, the color of the mini-emulsions changed from dark brown to milky brown. The observed transition was associated with the decrease in the amount of "free" GQDs located in the continuous phase because they were strongly adsorbed to the O/W interface as the thermal reduction time increased. Previously, it was reported that the GO-stabilized emulsion polymerization of styrene produced rough and textured surface morphology due to the large size of the GO sheet.[9,11] In contrast, as shown in Figures 4(c) and (d), the addition of rGQD5s produced relatively monodispersed, micron-sized, spherical, PS colloidal particles with smooth surfaces, which resembled the morphologies of the organic surfactant-stabilized particles.[49,50]

The self-assembly of block copolymers (BCPs) confined in the emulsion droplets can generate nanostructured particles with tunable internal structures and shapes, thus giving rise to potential applications in particle-based technologies, such as photonic bandgap materials, optical devices, and catalytic supports.[51−55] Therefore, in order to demonstrate the versatility of the GQD surfactants, we used them as stabilizers to produce symmetrical BCPs of polystyrene-*b*-polybutadiene (PS-*b*-PB) confined in the emulsion droplets. For the BCP particles, a 1 wt % toluene solution of PS-*b*-PB was emulsified in water that contained 10 mg of nGQDs and rGQD5s, respectively. When the nGQDs were added into the PS-*b*-PB emulsion, only an aggregated polymer sheet was found, as shown in Figure 5(a). In stark contrast, spherical particles with radially stacked, lamellar structures were fabricated when rGQD5s were used as the stabilizers (Figure 5(b)). The

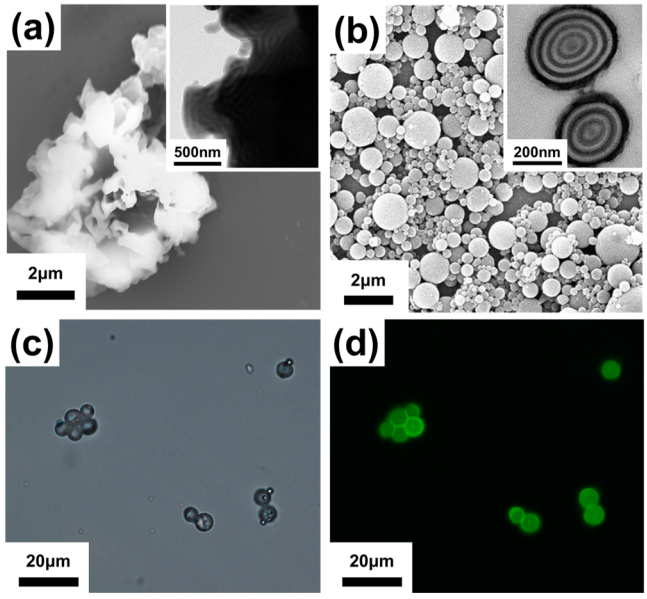

Figure 5. SEM images of PS-*b*-PB block copolymer (BCP) particles stabilized by (a) nGQDs and (b) rGQD5s. The inset figures are TEM images for each type of BCP emulsion. (c) Optical and (d) fluorescence microscopy images of PS-*b*-PB particles stabilized by rGQD5 as the surfactant. The excitation wavelength was 450 nm.

dx.doi.org/10.1021/mz5003855 | *ACS Macro Lett.* 2014, 3, 985−990

nGQDs have insufficient power to stabilize the particles, thus the emulsions coalesce and precipitate, forming aggregated polymer sheets. However, rGQD5s can stabilize the emulsions effectively and generate spherical particles, in which the symmetrical PS-*b*-PB polymers formed spherically confined, layered, "onion-like" internal structures (Figure 5(b)). Figures 5(c) and (d) show the optical and corresponding fluorescence microscopy images of PS-*b*-PB particles stabilized by rGQD5s. Interestingly, the dot-patterned luminescence in Figure 5(d) originated from the PS-*b*-PB particles stabilized by rGQD5. As a control sample, we fabricated the same BCP particles stabilized by another organic surfactant, i.e., cetyltrimethylammonium bromide (CTAB), and confirmed that there were no fluorescent emissions from the particles stabilized by CTAB (Figures S4(a) and (b), Supporting Information). Therefore, the BCP particles showed a strong, green emission as a result of the highly fluorescent GQDs' being distributed on the surfaces of the particles. These features provided a successful example of the synergistic combination of the unique properties of the thermally reduced GQDs into the emulsion droplets, providing their potential application in areas such as high contrast bioimaging and fluorescent sensors. Also, Figure S5 (Supporting Information) shows the optical and fluorescence microscopy images of cross-sectioned BCP particles, confirming that rGQD5s were strongly segregated at the surface of the BCP particles.

We demonstrated, for the first time, the surfactant-like behavior of 10 nm sized GQDs with tailored surface properties for producing highly stable O/W emulsion and polymer particles. The thermal reduction times of the GQDs were controlled to produce nGQDs, rGQD1s, and rGQD5s, which have the same sizes and heights but different level of hydrophobicities. In the O/W emulsion system, only the rGQD5 surfactants exhibited strong compatibilizing power due to their balanced amphiphilicity combined with their high surface area. These novel GQD surfactants were highly efficient for producing PS colloidal particles and PS-*b*-PB particles without any curvature effect due to their small size of 10 nm. Furthermore, we demonstrated that the remarkable optical properties of the GQDs can be combined synergistically with the emulsion droplets. For example, the GQD-stabilized BCP particles showed strong luminescence as the result of the highly fluorescent GQDs, thus offering great promise for their use in bioimaging and environmental applications.

■ ASSOCIATED CONTENT

Supporting Information

Materials and methods, detailed experimental procedures, and additional data. This material is available free of charge via the Internet at http://pubs.acs.org.

■ AUTHOR INFORMATION

Corresponding Author

*E-mail: bumjoonkim@kaist.ac.kr.

Notes

The authors declare no competing financial interest.

■ ACKNOWLEDGMENTS

This research was supported by the National Research Foundation Grant (2012R1A1A2A10041283, 2012M1A2A2671746), funded by the Korean Government. This work was also supported by Samsung Research Funding Center of Samsung Electronics under Project Number SRFC-MA1301-07. This research was supported by the New & Renewable Energy Program of KETEP Grant (20133030000130, 2011-T100100587), funded by the Ministry of Trade, industry & Energy, Republic of Korea. Authors also acknowledge the KAIST-KUSTAR Research Project for the financial support. We thank Soojeong Cho for the help in the fluorescence microscopy measurements. We also thank Lulu Ma, Sehmus Ozden, and Dr. Tharangattu N. Narayanan for helpful discussions.

■ REFERENCES

(1) Binks, B. P. *Curr. Opin. Colloid Interface Sci.* **2002**, *7*, 21−41.
(2) Aveyard, R.; Binks, B. P.; Clint, J. H. *Adv. Colloid Interfaces* **2003**, *100*, 503−546.
(3) Dinsmore, A. D.; Hsu, M. F.; Nikolaides, M. G.; Marquez, M.; Bausch, A. R.; Weitz, D. A. *Science* **2002**, *298*, 1006−1009.
(4) Vignati, E.; Piazza, R.; Lockhart, T. P. *Langmuir* **2003**, *19*, 6650−6656.
(5) Boker, A.; He, J.; Emrick, T.; Russell, T. P. *Soft Matter* **2007**, *3*, 1231−1248.
(6) Stratford, K.; Adhikari, R.; Pagonabarraga, I.; Desplat, J.-C.; Cates, M. E. *Science* **2005**, *309*, 2198−2201.
(7) Tu, F.; Park, B. J.; Lee, D. *Langmuir* **2013**, *29*, 12679−12687.
(8) Kim, J.; Cote, L. J.; Kim, F.; Yuan, W.; Shull, K. R.; Huang, J. *J. Am. Chem. Soc.* **2010**, *132*, 8180−8186.
(9) Thickett, S. C.; Zetterlund, P. B. *ACS Macro Lett.* **2013**, *2*, 630−634.
(10) He, Y.; Wu, F.; Sun, X.; Li, R.; Guo, Y.; Li, C.; Zhang, L.; Xing, F.; Wang, W.; Gao, J. *ACS Appl. Mater. Interfaces* **2013**, *5*, 4843−4855.
(11) Che Man, S. H.; Thickett, S. C.; Whittaker, M. R.; Zetterlund, P. B. *J. Polym. Sci., Part A: Polym. Chem.* **2013**, *51*, 47−58.
(12) McCoy, T. M.; Pottage, M. J.; Tabor, R. F. *J. Phys. Chem. C* **2014**, *118*, 4529−4535.
(13) Sun, Z.; Feng, T.; Russell, T. P. *Langmuir* **2013**, *29*, 13407−13413.
(14) Kim, F.; Cote, L. J.; Huang, J. *Adv. Mater.* **2010**, *22*, 1954−1958.
(15) Ikem, V. O.; Menner, A.; Bismarck, A. *Angew. Chem., Int. Ed.* **2008**, *47*, 8277−8279.
(16) Chung, H.-J.; Ohno, K.; Fukuda, T.; Composto, R. J. *Nano Lett.* **2005**, *5*, 1878−1882.
(17) Kubowicz, S.; Daillant, J.; Dubois, M.; Delsanti, M.; Verbavatz, J. M.; Mohwald, H. *Langmuir* **2010**, *26*, 1642−1648.
(18) Kwon, T.; Kim, T.; Ali, F. B.; Kang, D. J.; Yoo, M.; Bang, J.; Lee, W.; Kim, B. J. *Macromolecules* **2011**, *44*, 9852−9862.
(19) Kang, D. J.; Kwon, T.; Kim, M. P.; Cho, C. H.; Jung, H.; Bang, J.; Kim, B. J. *ACS Nano* **2011**, *5*, 9017−9027.
(20) Jang, S. G.; Audus, D. J.; Klinger, D.; Krogstad, D. V.; Kim, B. J.; Cameron, A.; Kim, S. W.; Delaney, K. T.; Hur, S. M.; Killops, K. L.; Fredrickson, G. H.; Kramer, E. J.; Hawker, C. J. *J. Am. Chem. Soc.* **2013**, *135*, 6649−6657.
(21) Voorn, D. J.; Ming, W.; van Herk, A. M. *Macromolecules* **2006**, *39*, 2137−2143.
(22) Miesch, C.; Kosif, I.; Lee, E.; Kim, J. K.; Russell, T. P.; Hayward, R. C.; Emrick, T. *Angew. Chem., Int. Ed.* **2012**, *51*, 145−149.
(23) Walther, A.; Matussek, K.; Muller, A. H. E. *ACS Nano* **2008**, *2*, 1167−1178.
(24) Chung, H.-J.; Kim, J.; Ohno, K.; Composto, R. J. *ACS Macro Lett.* **2012**, *1*, 252−256.
(25) Chen, T.; Colver, P. J.; Bon, S. A. F. *Adv. Mater.* **2007**, *19*, 2286−2289.
(26) Kwon, T.; Ku, K. H.; Kang, D. J.; Lee, W. B.; Kim, B. J. *ACS Macro Lett.* **2014**, *3*, 398−404.
(27) Zhang, Z.; Zhang, J.; Chen, N.; Qu, L. *Energy Environ. Sci.* **2012**, *5*, 8869−8890.
(28) Cheng, H.; Zhao, Y.; Fan, Y.; Xie, X.; Qu, L.; Shi, G. *ACS Nano* **2012**, *6*, 2237−2244.
(29) Zhuo, S.; Shao, M.; Lee, S. T. *ACS Nano* **2012**, *6*, 1059−1064.

(30) Zheng, X. T.; Than, A.; Ananthanaraya, A.; Kim, D. H.; Chen, P. *ACS Nano* **2013**, *7*, 6278−6286.
(31) Jin, S. H.; Kim, D. H.; Jun, G. H.; Hong, S. H.; Jeon, S. *ACS Nano* **2013**, *7*, 1239−1245.
(32) Guo, C. X.; Dong, Y.; Yang, H. B.; Li, C. M. *Adv. Energy Mater.* **2013**, *3*, 997−1003.
(33) Li, Y.; Hu, Y.; Zhao, Y.; Shi, G.; Deng, L.; Hou, Y.; Qu, L. *Adv. Mater.* **2011**, *23*, 776−780.
(34) Pan, D.; Zhang, J.; Li, Z.; Wu, M. *Adv. Mater.* **2010**, *22*, 734−738.
(35) Peng, J.; Gao, W.; Gupta, B. K.; Liu, Z.; Romero-Aburto, R.; Ge, L.; Song, L.; Alemany, L. B.; Zhan, X.; Gao, G.; Vithayathil, S. A.; Kaipparettu, B. A.; Marti, A. A.; Hayashi, T.; Zhu, J.; Ajayan, P. M. *Nano Lett.* **2012**, *12*, 844−849.
(36) Zhu, S.; Zhang, J.; Qiao, C.; Tang, S.; Li, Y.; Yuan, W.; Li, B.; Tian, L.; Liu, F.; Hu, R.; Gao, H.; Wei, H.; Zhang, H.; Sun, H.; Yang, B. *Chem. Commun.* **2011**, *47*, 6858−6860.
(37) Kim, J. K.; Park, M. J.; Kim, S. J.; Wang, D. H.; Cho, S. P.; Bae, S.; Park, J. H.; Hong, B. H. *ACS Nano* **2013**, *7*, 7207−7212.
(38) Gupta, V.; Chaudhary, N.; Srivastava, R.; Sharma, G. D.; Bhardwaj, R.; Chand, S. *J. Am. Chem. Soc.* **2011**, *133*, 9960−9963.
(39) Zhu, S.; Zhang, J.; Tang, S.; Qiao, C.; Wang, L.; Wang, H.; Liu, X.; Li, B.; Li, Y.; Yu, W.; Wang, X.; Sun, H.; Yang, B. *Adv. Funct. Mater.* **2012**, *22*, 4732−4740.
(40) Yang, H.; Kwon, Y.; Kwon, T.; Lee, H.; Kim, B. J. *Small* **2012**, *8*, 3161−3168.
(41) Paek, K.; Yang, H.; Lee, J.; Park, J.; Kim, B. J. *ACS Nano* **2014**, *8*, 2848−2856.
(42) Dreyer, D. R.; Park, S.; Bielawski, C. W.; Ruoff, R. S. *Chem. Soc. Rev.* **2010**, *39*, 228−240.
(43) Zhu, Y.; Murali, S.; Cai, W.; Li, X.; Suk, J. W.; Potts, J. R.; Ruoff, R. S. *Adv. Mater.* **2010**, *22*, 3906−3924.
(44) Dong, Y.; Chen, C.; Zheng, X.; Gao, L.; Cui, Z.; Yang, H.; Guo, C.; Chi, Y.; Li, C. M. *J. Mater. Chem.* **2012**, *22*, 8764−8766.
(45) Compton, O. C.; Jain, B.; Dikin, D. A.; Abouimrane, A.; Amine, K.; Nguyen, S. T. *ACS Nano* **2011**, *5*, 4380−4391.
(46) Villar-Rodil, S.; Paredes, J. I.; Martinez-Alonso, A.; Tascon, J. M. D. *J. Mater. Chem.* **2009**, *19*, 3591−3593.
(47) Pieranski, P. *Phys. Rev. Lett.* **1980**, *45*, 569−572.
(48) Niu, Z.; He, J.; Russell, T. P.; Wang, Q. *Angew. Chem., Int. Ed.* **2010**, *49*, 10052−10066.
(49) Gabaston, L. I.; Jackson, R. A.; Armes, S. P. *Macromolecules* **1998**, *31*, 2883−2888.
(50) Landfester, K.; Bechthold, N.; Tiarks, F.; Antonietti, M. *Macromolecules* **1999**, *32*, 2679−2683.
(51) Arsenault, A. C.; Rider, D. A.; Tétreault, N.; Chen, J. I. L.; Coombs, N.; Ozin, G. A.; Manners, I. *J. Am. Chem. Soc.* **2005**, *127*, 9954−9955.
(52) Jeon, S. J.; Yi, G. R.; Yang, S. M. *Adv. Mater.* **2008**, *20*, 4103−4108.
(53) Li, L.; Matsunaga, K.; Zhu, J.; Higuchi, T.; Yabu, H.; Shimomura, M.; Jinnai, H.; Hayward, R. C.; Russell, T. P. *Macromolecules* **2010**, *43*, 7807−7812.
(54) Kim, M. P.; Kang, D. J.; Jung, D. W.; Kannan, A. G.; Kim, K. H.; Ku, K. H.; Jang, S. G.; Chae, W. S.; Yi, G. R.; Kim, B. J. *ACS Nano* **2012**, *6*, 2750−2757.
(55) Ku, K. H.; Shin, J. M.; Kim, M. P.; Lee, C.-H.; Seo, M.-K.; Yi, G.-R.; Jang, S. G.; Kim, B. J. *J. Am. Chem. Soc.* **2014**, *136*, 9982−9989.